

UC Santa Barbara

UC Santa Barbara Previously Published Works

Title

Synthesis and Properties of Quinoxaline-Containing Benzoxazines and Polybenzoxazines

Permalink

<https://escholarship.org/uc/item/30k161gs>

Journal

ACS Omega, 4(5)

ISSN

2470-1343

Authors

Chen, Chien Han
Yu, Tsung Yen
Wu, Jen-Hao
[et al.](#)

Publication Date

2019-05-31

DOI

10.1021/acsomega.9b01042

Peer reviewed

Synthesis and Properties of Quinoxaline-Containing Benzoxazines and Polybenzoxazines

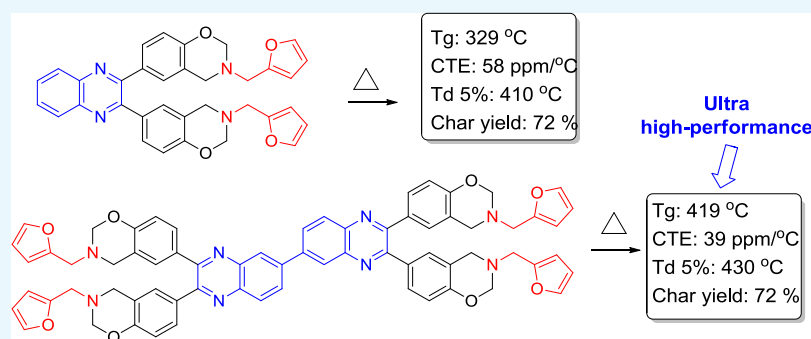
Chien Han Chen,[†] Tsung Yen Yu,[‡] Jen-Hao Wu,^{||} Mathivathanan Ariraman,[‡] Tzong-Yuan Juang,^{*,§} Mahdi M. Abu-Omar,[⊥] and Ching-Hsuan Lin^{*,†,‡,⊥}

[†]Advanced Research Center for Green Materials Science and Technology, National Taiwan University, Taipei 10617, Taiwan

[‡]Department of Chemical Engineering, National Chung Hsing University, Taichung 402, Taiwan

[§]Department of Cosmeceutics and ^{||}School of Pharmacy, China Medical University, Taichung 404, Taiwan

[⊥]Department of Chemistry and Biochemistry, University of California, Santa Barbara, Santa Barbara, California 93106, United States



ABSTRACT: The object of this work is to prepare quinoxaline-based benzoxazines and evaluate thermal properties of their thermosets. For this object, 4,4'-(quinoxaline-2,3-diyl)diphenol (QDP)/furfurylamine-based benzoxazine (QDP-fu) and 4,4',4'',4'''-([6,6'-biquinoxaline]-2,2',3,3'-tetrayl)tetraphenol (BQTP)/furfurylamine-based benzoxazine (BQTP-fu) were prepared. The structures of QDP-fu and BQTP-fu were successfully confirmed by FTIR and ¹H and ¹³C NMR spectra. We studied the curing behavior of QDP-fu and BQTP-fu and thermal properties of their thermosets. According to DSC thermograms, QDP-fu and BQTP-fu have the attractive onset exothermic temperatures of 181 and 186 °C, respectively. The onset temperature is approximately 45 °C lower than that of a bisphenol A/furfurylamine-based benzoxazines. According to DMA TMA and TGA thermograms, the thermoset of BQTP-fu shows impressive thermal properties, with a T_g value of 418 °C, a coefficient of thermal expansion of 39 ppm/°C, a 5% decomposition temperature of 430 °C, and a char yield of 72%.

1. INTRODUCTION

Quinoxaline, a complex ring of benzene and pyrazine, is generally formed by the condensation of an *ortho*-diamine with a dialdehyde,¹ ethanol,² 1,4-dioxane-2,3-diol,³ and so on. Polyquinoxalines, prepared by the reaction of a bis(*o*-diamine) with a bisglyoxal⁴ or a bisbenzil,⁵ are a class of high-performance polymers with many attractive properties, including excellent hydrolytic, thermal, and mechanical properties. In addition, quinoxaline derivatives have shown antibacterial, antiviral, herbicidal, anti-inflammatory, and antitumor properties.^{6–13}

Benzoxazine are heterocyclic compounds and will proceed ring-opening polymerization (ROP) during thermal treatment.^{14–20} Benzoxazine thermosets have unique properties such as moderate-to-high thermal properties and dimensional stability, and low surface free energy.^{21,22} The properties of benzoxazine thermosets are strongly influenced by the structures of their precursors. Because polyquinoxalines are a class of high-performance polymers, benzoxazines with quinoxaline as a core might result in high performance. However, to the best of our knowledge, the literature on

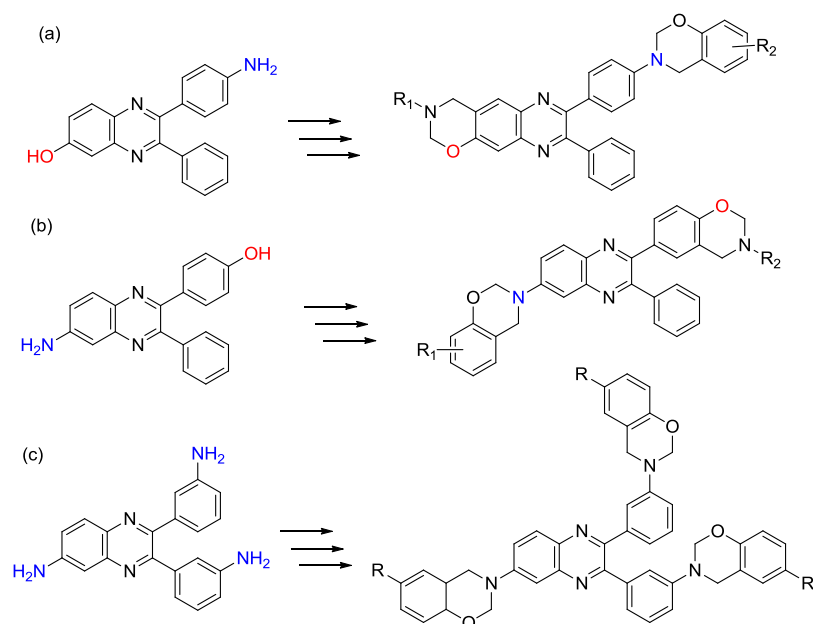
quinoxaline-containing 1,3-benzoxazines is rare and limited to three patents.^{23–25} Wang et al. prepared benzoxazines from a quinoxaline-containing aminophenol (Scheme 1a),²³ aminophenol (Scheme 1b),²⁴ and triamine (Scheme 1c).²⁵ The benzoxazine thermosets show T_g values as high as 195, 213, and 372 °C, respectively. Generally, it is difficult to prepare a benzoxazine monomer from an aminophenol because it is an A–B type reactant, and will lead to oligomeric benzoxazines.²⁶ In addition, it is difficult to prepare a benzoxazine monomer from triamine because the reaction of triamine with formaldehyde led to a triazine network and resulted in gelation.²⁷ To avoid these problems, the authors use a three-step procedure to prepare the desired benzoxazine monomers.²⁸ Although high-purity benzoxazines can be prepared through that approach, multiple steps (at least four) are required to prepare the aforementioned quinoxaline-containing 1,3-benzoxazines.

Received: April 11, 2019

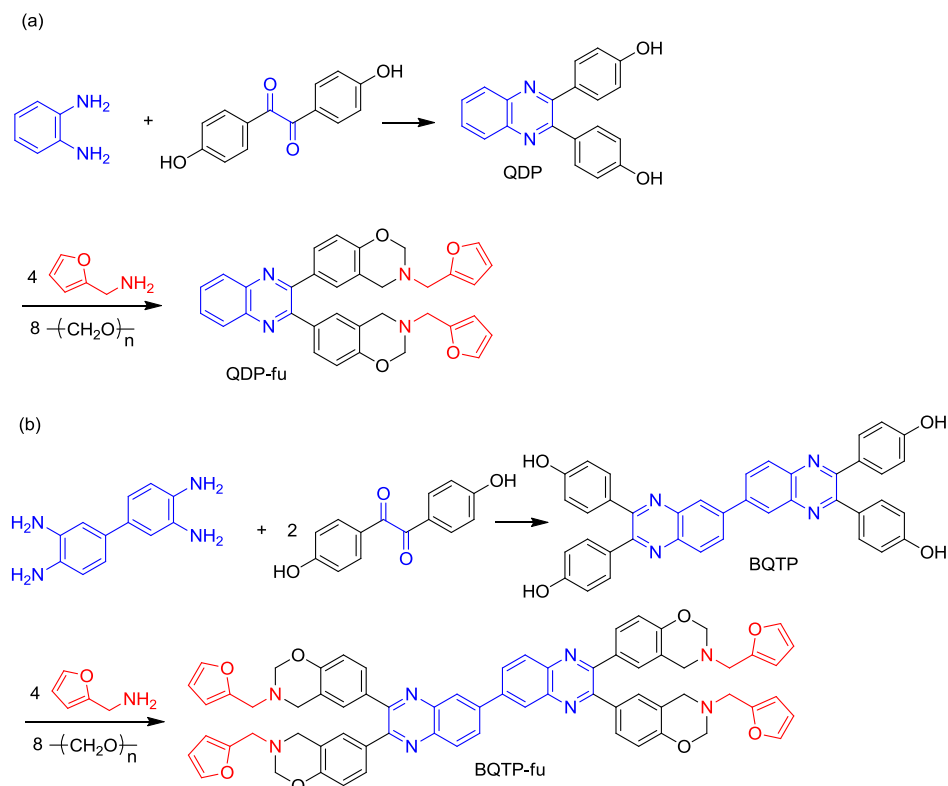
Accepted: May 7, 2019

Published: May 23, 2019

Scheme 1. Synthesis of a Quinoxaline-Containing Benzoxazine from (a) Aminophenol,²³ (b) Aminophenol,²⁴ and (c) Triamine²⁵ by a Three-Step Procedure²⁸



Scheme 2. Synthesis of (a) QDP and QDP-fu (b) BQTP and BQTP-fu



Furfurylamine is typically formed by the amination of furfural, which is a product of acid-catalyzed dehydration of 5-carbon sugars,²⁹ and is one of the oldest renewable chemicals.³⁰ Furfurylamine-containing benzoxazines received much attention because of their low cost and high performance. For example, Liu et al. prepared a bisphenol A/furfurylamine-based benzoxazine and found that the reaction between furan and oxazine increased the thermal stability.³¹ Verge et al. prepared benzoxazines from phloretic acid-derived

biphenols and furfurylamine.³² The work highlighted the suitability of phloretic acid to act as a green and efficient alternative to phenol. Endo et al. prepared guaiacol/furfurylamine-based benzoxazine, they reported that the furan moiety participates in the ROP of benzoxazines via electrophilic aromatic substitution.³³ Varma et al. prepared a vanillin/furfurylamine-based benzoxazine.³⁴ A curing mechanism of furan electrophilic substitution and decarboxylation was proposed. Dumas et al. prepared resorcinol/furfurylamine-

based and hydroquinone/furfurylamine-based benzoxazines by a solventless method. The thermosets exhibit excellent thermomechanical properties with glass transition temperatures higher than 280 °C and present remarkable inherent charring ability upon pyrolysis.³⁵ Dumas et al. also prepared a water-soluble arbutin/furfurylamine-based benzoxazine in a solventless method. Thermoset with a T_g of 190 °C and good adhesion on various substrates was achieved.³⁶ Liu et al. prepared a daidzein/furfurylamine-based bio-benzoxazine through a microwave-assisted synthesis in PEG 400.³⁷ According to the literature, a thermoset with a T_g of 391 °C dynamic mechanical analysis (DMA data), the highest T_g value that has ever reported at that time, was achieved.

In this work, we report the facile synthesis two quinoxaline-containing benzoxazines. The first one is a difunctional benzoxazine (QDP-fu), prepared from the Mannich condensation of furfurylamine, formaldehyde, and 4,4'-(quinoxaline-2,3-diyl)diphenol (QDP). The second one is a tetrafunctional benzoxazine (BQTP-fu) from the Mannich condensation of furfurylamine, formaldehyde, and 4,4',4'',4'''-([6,6'-biquinoxaline]-2,2',3,3'-tetrayl)tetraphenol (BQTP). We studied the curing behavior of QDP-fu and BQTP-fu and thermal properties of their thermosets. Detailed synthesis and characterization of QDP-fu and BQTP-fu and the properties of their thermosets were analyzed in this work.

2. RESULTS AND DISCUSSION

2.1. Synthesis and Characterization of QDP and BQTP.

The biphenol (QDP) was prepared from the condensation of 4,4-dihydroxybenzil with *o*-phenylenediamine. The tetraphenol (BQTP) was prepared from the condensation of 4,4-dihydroxybenzil with 3,3'-diaminobenzidine (Scheme 2). Figure 1 shows the ^1H - ^{13}C HETCOR NMR spectra of (a) QDP and (b) BQTP. The correlation in Figure 1 supports the structure of QDP and BQTP.

Synthesis and Characterization of QDP-fu and BQTP-fu.

According to the literature,³⁸ benzoxazine synthesis is proceeded by two steps: the formation of triazine and the dissociation of the resulting triazine. In our previous work,³⁹ we found that the solvents influence the reaction rate of the two steps, and the co-solvent of toluene/ethanol works best for the synthesis of benzoxazine. QDP-fu was synthesized from the Mannich condensation of furfurylamine, formaldehyde, and QDP (Scheme 2). Table 1 (Runs 1–6) lists the effect of reaction conditions on the preparation of QDP-fu. Reacting in 1,4-dioxane (Run 1), a common solvent for Mannich condensation, at 80 °C for 12 h led to low conversion and low yield. Reacting in dioxane/ethanol at 85–95 °C (Runs 2–4) and toluene/ethanol at 80 °C (Runs 5), a recommended medium for Mannich condensation in our previous work,³⁹ also led to an incomplete reaction with low yield. We think that the conjugation of phenol with quinoxaline reduced the reactivity (Scheme 3). Therefore, a solvent with a higher boiling point was considered. Xylene was chosen to replace toluene, and 1-pentanol was chosen to replace ethanol. Reacting in xylene/1-pentanol at 120 °C (Run 6), as expected, led to a complete reaction and an 85% yield. BQTP-fu can also be successfully synthesized in xylene/pentanol at 120 °C from the Mannich condensation of furfurylamine, formaldehyde, and BQTP (Scheme 2). Because of the resonance of phenol and C=N of quinoxaline that will reduce the electron density of the phenol group in QDP and BQTP, the preparation of QDP-fu and BQTP-fu is not as easy as a bisphenol A/

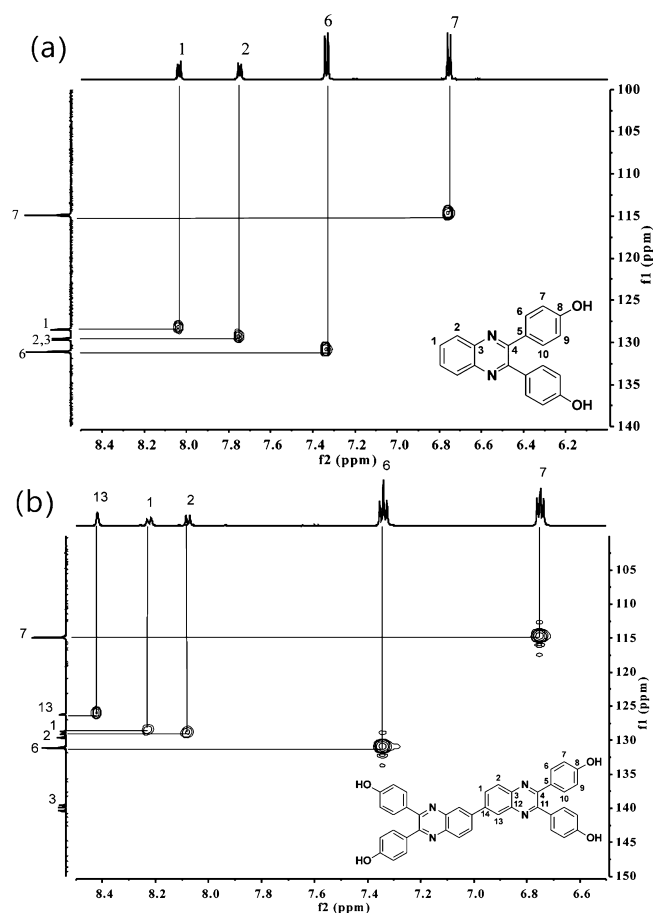
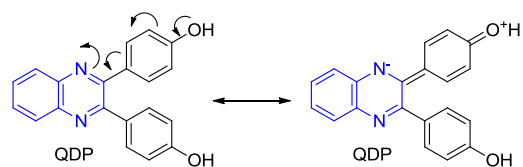


Figure 1. Enlarged ^1H - ^{13}C HETCOR NMR spectrum of (a) QDP and (b) BQTP.

Table 1. Reaction Conditions on the Synthesis of QDP-fu

run	solvent	reaction conditions (temp, concentration)	result
1	dioxane	85 °C, 0.1 g/mL	incomplete reaction (yield <25%)
2	dioxane/ethanol (1:1)	85 °C, 0.1 g/mL	incomplete reaction (yield <25%)
3	dioxane/1-propanol (1:2)	95 °C, 0.1 g/mL	incomplete reaction (yield <25%)
4	dioxane/1-propanol (2:1)	95 °C, 0.1 g/mL	incomplete reaction (yield <40%)
5	toluene/ethanol (2:1)	80 °C, 0.1 g/mL	incomplete reaction (yield <40%)
6	xylene/1-pentanol (2:1)	120 °C, 0.1 g/mL	pure product (yield 85%)

Scheme 3. Conjugation of Phenol with Quinoxaline



furfurylamine-based benzoxazine. Therefore, the high-boiling co-solvent of xylene/1-pentanol that can provide high reaction temperature at 120 °C, works the best.

Figure 2 shows the ^1H NMR spectrum of QDP and QDP-fu. For the QDP-fu, no phenolic hydroxyl at 9.8 ppm was observed, indicating the completion of the reaction. The

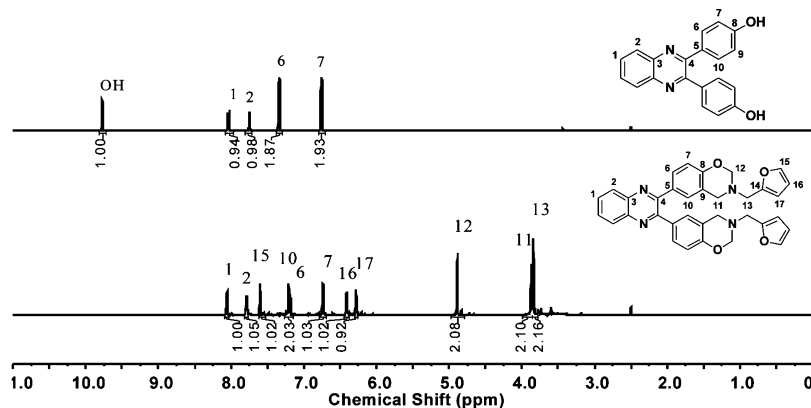


Figure 2. ^1H NMR spectra of QDP and QDP-fu in $\text{DMSO-}d_6$.

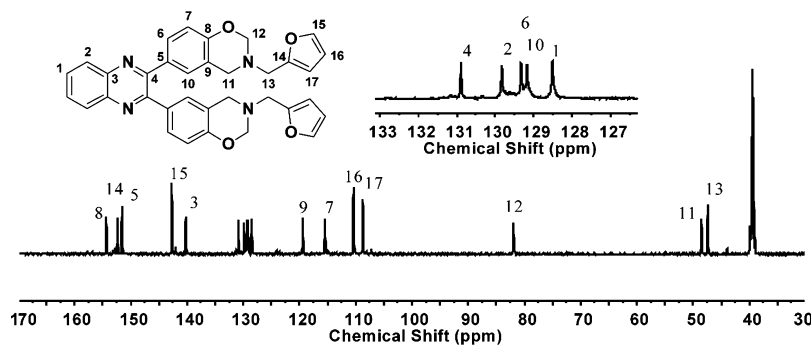


Figure 3. ^{13}C NMR spectrum of QDP-fu.

characteristic peaks at 7.6, 6.4, and 6.2 ppm (H^{15} – H^{17} for furan), 4.89 and 3.87 ppm (H^{12} and H^{11} for oxazine) confirm the structure of QDP-fu. Figure 3 shows the ^{13}C NMR spectrum of QDP-fu. The characteristic peaks at 152.4, 142.7, 110.4, and 108.7 ppm (C^{14} – C^{17} for furan), 81.2 and 48.5 ppm (C^{12} and C^{11} for oxazine) confirm the structure of QDP-fu. Figure 4 shows the enlarged (a) ^1H – ^1H COSY and (b) ^1H – ^{13}C HETCOR NMR spectra of QDP-fu. The correlation of NMR signals is consistent with the structure of QDP-fu.

Figure 5 shows the ^1H NMR spectrum of BQTP and BQTP-fu. For BQTP-fu, no phenolic hydroxyl at 9.8 ppm was observed, indicating the completion of the reaction. The characteristic peaks at 7.6, 6.4, and 6.2 ppm (H^{19} – H^{21} for furan), 4.89 and 3.8 ppm (H^{15} and H^{16} for oxazine) confirm the structure of BQTP-fu. Figure 6 shows the ^{13}C NMR spectrum of BQTP-fu. The characteristic peaks at 152.4, 142.7, 110.4, and 108.7 ppm (C^{18} – C^{21} for furan), 82.0 and 48.5 ppm (C^{16} and C^{15} for oxazine) confirm the structure. Figure 7 shows the enlarged (a) ^1H – ^1H COSY and (b) ^1H – ^{13}C HETCOR NMR spectra of BQTP-fu. The assignments of NMR signals are consistent with the structure of BQTP-fu.

2.2. DSC Thermograms. Figure 8 displays the differential scanning calorimetry (DSC) thermograms of QDP-fu and BQTP-fu. QDP-fu and BQTP-fu, respectively, show a melting point at 65 and 102 $^\circ\text{C}$, and an onset exothermic temperature approximately at 202 and 204 $^\circ\text{C}$ and an enthalpy of 359 and 172 kJ/mol, respectively. The onset exothermic temperature is approximately 25 $^\circ\text{C}$ lower than that of bisphenol A/furfurylamine-based benzoxazine (BA-fu).³¹ We prepared the 4,4'-bisphenol F/furfurylamine-based benzoxazine (BF-fu) for comparison of the DSC thermogram (Figure 8). The onset exothermic temperature is approximately 18 $^\circ\text{C}$ higher than

that of QDP-fu. We speculate that the lone pair of nitrogen of quinoxaline might play a role in catalyzing the ring opening of oxazine. It probably explains the lower onset exothermic temperatures of QDP-fu and BQTP-fu than those of BA-fu and BF-fu. However, a detailed analysis is required to confirm for the speculation. The exothermic peaks of QDP-fu and BQTP-fu are different from general benzoxazines. They are not symmetrical and seem to be the combination of two exothermic peaks. The same result was also observed for BF-fu. From IR analysis (Figure 10, to be discussed later), we found sequential curing reactions for QDP-fu and BQTP-fu. The sequential curing reactions probably explain the two exothermic peaks of QDP-fu, BQTP-fu, and BF-fu.

2.3. Rheology Curves. Figure 9 shows the isothermal rheology curves of QDP-fu and BQTP-fu at 180 $^\circ\text{C}$. The gelation time was determined by the moduli cross-over point in the isothermal, isochronic curves. QDP-fu has a gelation time of 25.1 min, while BQTP-fu, because of its tetrafunctional characteristic, has a shorter gelation time of 11.1 min.

2.4. IR Analysis. Referring to the curing chemistry of furan and benzoxazine,^{33,40} three reaction routes for the curing of QDP-fu are shown in Scheme 4. The first route is the ring opening of benzoxazine, forming an intermediate with zwitterions of oxazine. The second route is the reaction of furan and the zwitterion of oxazine, leading to structure 2. The third route is the reaction of free ortho and zwitterion of oxazine, leading to structure 3. FTIR was used to monitor the curing reactions. Figure 10a shows the IR spectra of QDP-fu after thermal treatment for 20 min at each temperature. As curing progressed, the absorption at 930 cm^{-1} (C–H out-of-plane bending absorption of oxazine) decreased remarkably. The signal of the trisubstituted benzene ring^{31,41,42} at 1501

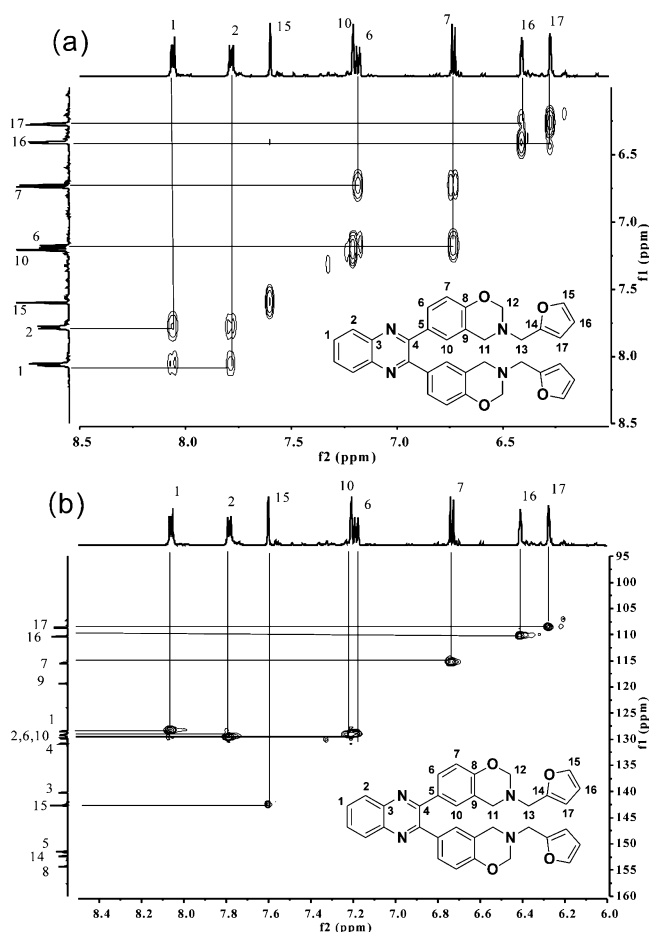


Figure 4. Enlarged (a) ^1H – ^1H COSY and (b) ^1H – ^{13}C HETCOR NMR spectra of QDP-fu in $\text{DMSO-}d_6$.

cm^{-1} decreased gradually with the curing temperature. This result confirms the curing of oxazine during the heating process. The signal of furan⁴⁰ at 985 cm^{-1} decreased gradually and disappeared after curing at $200\text{ }^\circ\text{C}$. The decrease of the signals of furan and the trisubstituted benzene ring at the early stages of curing supports the reaction routes 1–2 shown in Scheme 4. The signal of the tetrasubstituted benzene ring^{31,33,40}

at 1477 cm^{-1} , which resulted from structure 3 shown in Scheme 4, increased gradually after curing at $200\text{ }^\circ\text{C}$. Therefore, the IR results indicate that routes 1,2 occurred at a lower temperature (before $180\text{ }^\circ\text{C}$), and route 2 occurred at a higher temperature (after $200\text{ }^\circ\text{C}$). Figure 10b shows the IR spectra of BQTP-fu after thermal treatment for 20 min at each temperature. The analytic result of BQTP-fu is the same as that of QDP-fu. We think that the sequence reactions are responsible for the two exothermic peaks of QDP-fu and BQTP-fu in the DSC thermograms of QDP-fu and BQTP-fu (Figure 8).

2.5. Thermal Properties. Figure 11 shows the thermal mechanical analysis (TMA) thermograms of QDP and BQTP after curing at 220 or $240\text{ }^\circ\text{C}$. The thermosets are named C-QDP-fu- X and C-BQTP-fu- X , in which X is the final curing temperature. The TMA result is listed in Table 2. Curing at $240\text{ }^\circ\text{C}$ lead to thermosets with a higher T_g than curing at $220\text{ }^\circ\text{C}$. For example, C-QDP-fu-240 and C-BQTP-fu-240 have a T_g value of 268 and $295\text{ }^\circ\text{C}$, respectively, which are about $30\text{ }^\circ\text{C}$ higher than those of C-QDP-fu-220 and C-BQTP-fu-220. Therefore, the final curing temperature of all samples is set to $240\text{ }^\circ\text{C}$, and the sample ID is named C-QDP-fu and C-BQTP-fu (we delete the “–240” for simplicity). TMA data show that thermoset based on tetrafunctional BQTP-fu has a higher T_g value and lower coefficient of thermal expansion (CTE) than that based on difunctional QDP-fu. For example, the T_g and CTE value of C-BQTP-fu are $298\text{ }^\circ\text{C}$ and $39\text{ ppm}/^\circ\text{C}$, which are better than those of C-QDP-fu ($268\text{ }^\circ\text{C}$ and $58\text{ ppm}/^\circ\text{C}$), demonstrating the advantage of tetrafunctional characteristic.

Figure 12 shows the DMA thermograms of C-QDP-fu and C-BQTP-fu. C-BQTP-fu, derived from tetrafunctional BQTP-fu, shows higher modulus (4.0 GPa) than the C-QDP-fu do (1.3 GPa). The T_g taken from the peak temperatures of $\tan\delta$ are 329 and $419\text{ }^\circ\text{C}$, respectively. The value of $329\text{ }^\circ\text{C}$ is similar to the T_g value of thermoset of difunctional bisphenol A/furfurylamine-based benzoxazine.³¹ However, the T_g value of $419\text{ }^\circ\text{C}$, to the best of our knowledge, is an ultra-high value for a benzoxazine thermoset. The tetrafunctional characteristic and the furan moiety that increase the cross-linking density explain the very high T_g characteristic.

Figure 13 and Table 2 show the thermogravimetric analysis (TGA) data of C-QDP-fu and C-BQTP-fu. The 5%

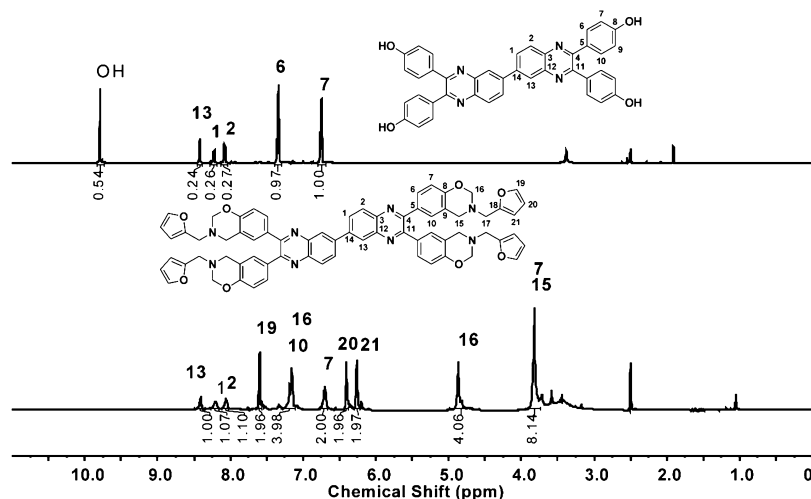


Figure 5. ^1H NMR spectra of BQTP and BQTP-fu in $\text{DMSO-}d_6$.

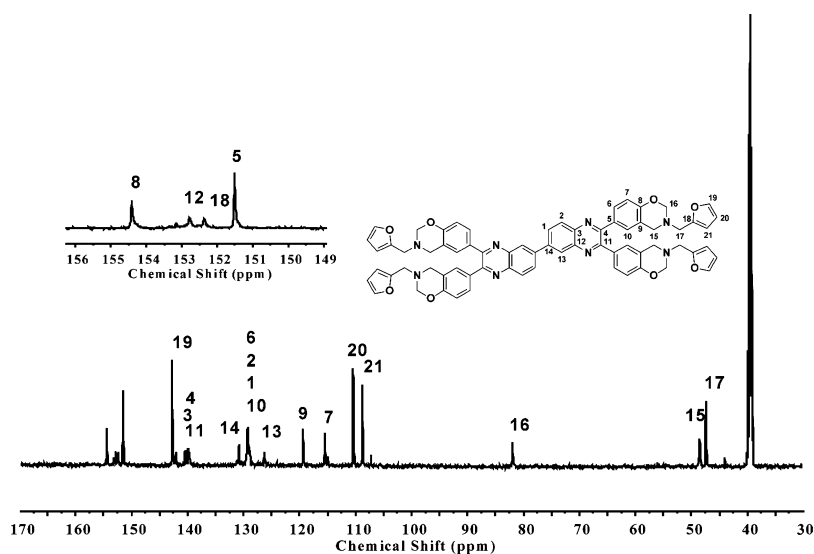


Figure 6. ^{13}C NMR spectrum of BQTP-fu.

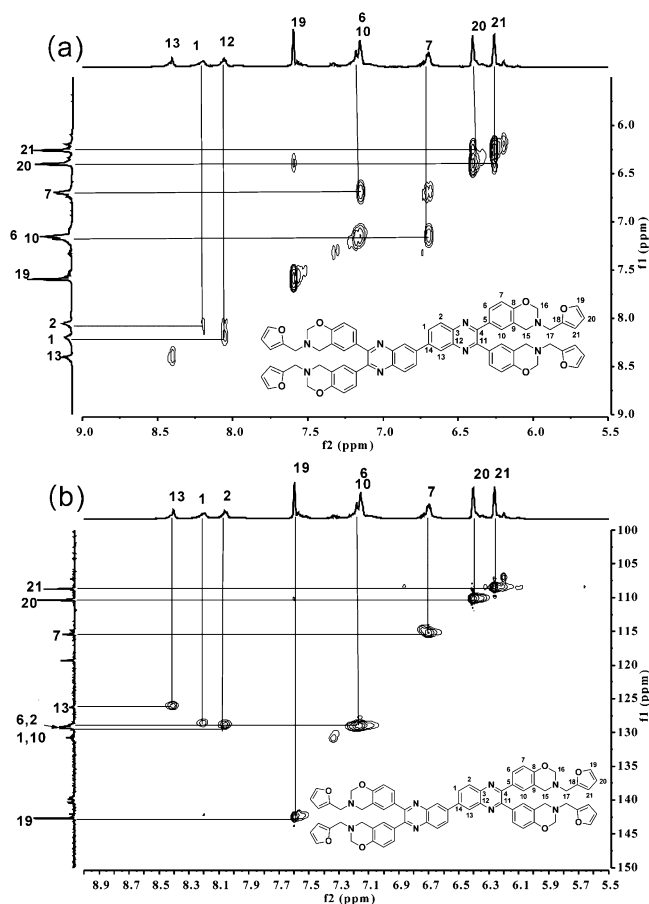


Figure 7. Enlarged (a) ^1H - ^1H COSY and (b) ^1H - ^{13}C HETCOR NMR spectra of BQTP-fu in $\text{DMSO}-d_6$.

decomposition temperatures for C-QDP-fu and C-BQTP-fu are 410 and 430 $^\circ\text{C}$, respectively. C-BQTP-fu shows a slightly higher decomposition temperature than C-QDP-fu, probably because of the higher functionality in the precursor. The char yield is as high as 72% for both C-QDP-fu and C-BQTP-fu. Generally, the thermost of bisphenol-based benzoxazines such as bisphenol F/aniline-based, and bisphenol A/aniline-based

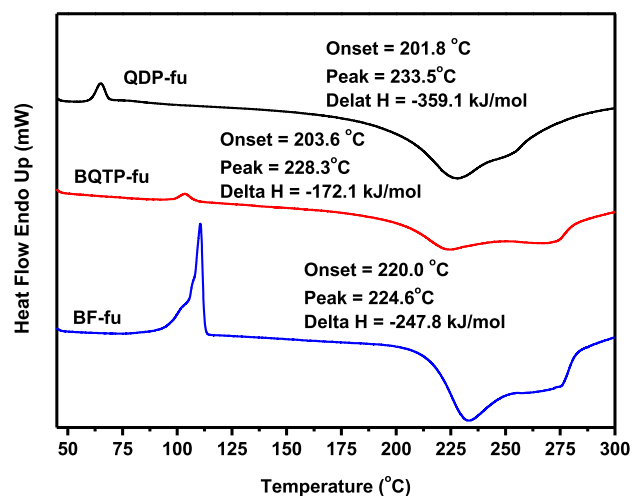


Figure 8. DSC heating thermograms of QDP-fu and BQTP-fu.

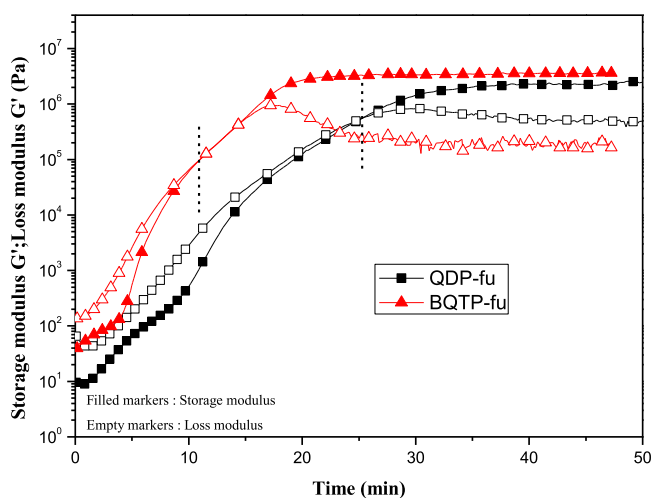


Figure 9. Isothermal rheology curves of QDP-fu and BQTP-fu at 180 $^\circ\text{C}$.

Scheme 4. Curing Chemistry for QDP-fu

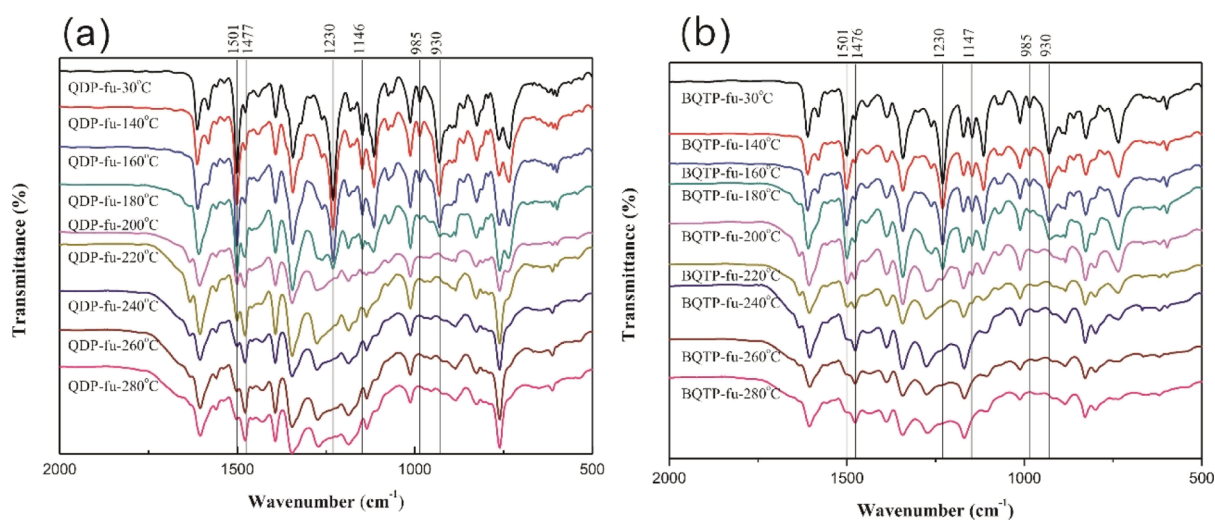
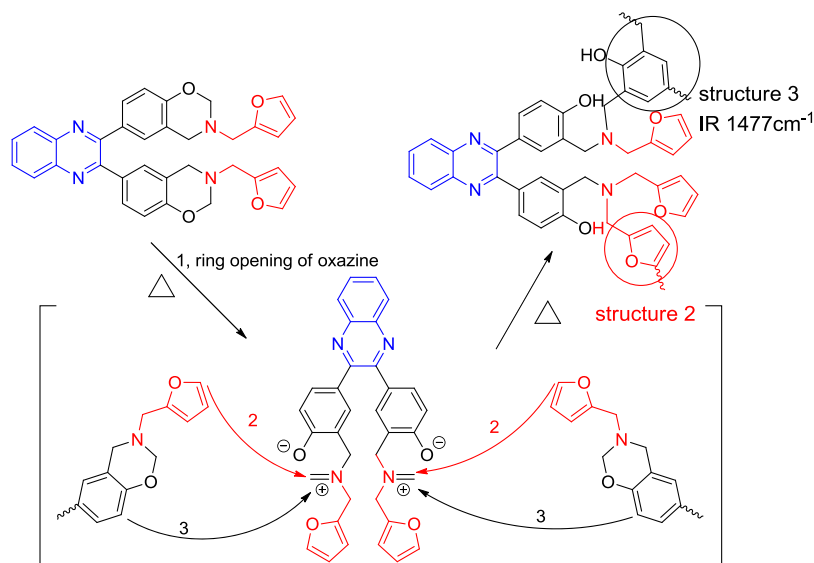


Figure 10. FTIR spectra of (a) QDP-fu and (b) BQTP-fu during curing process.

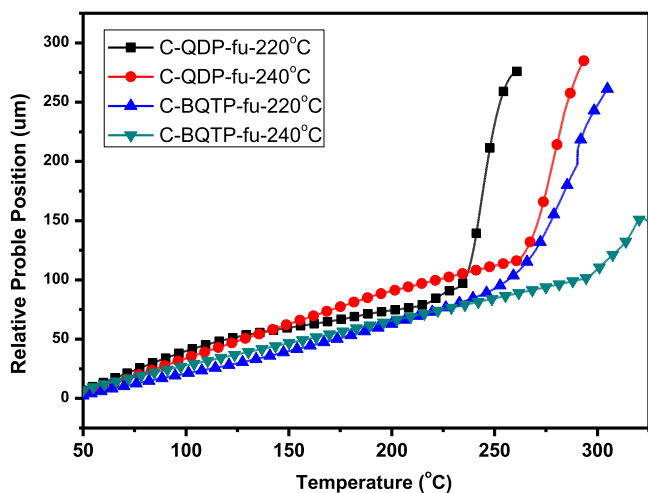


Figure 11. TMA thermograms of C-QDP-fu-X and C-BQTP-fu-X.

benzoxazine exhibit a 5 wt % decomposition temperature at around 300–350 °C.^{43,44} The result demonstrates the high thermal stability characteristic of C-QDP-fu and C-BQTP-fu.

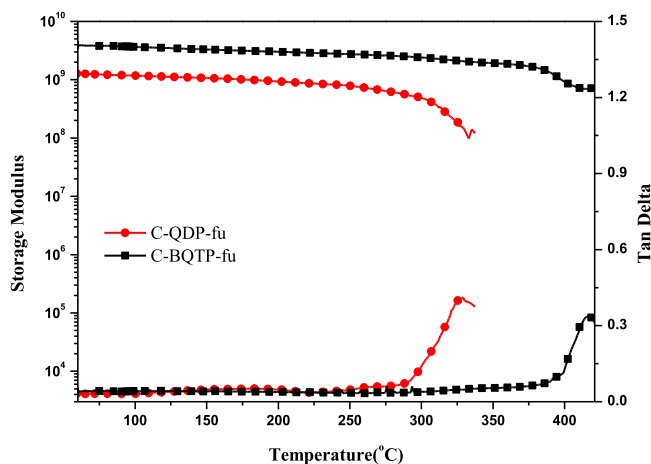
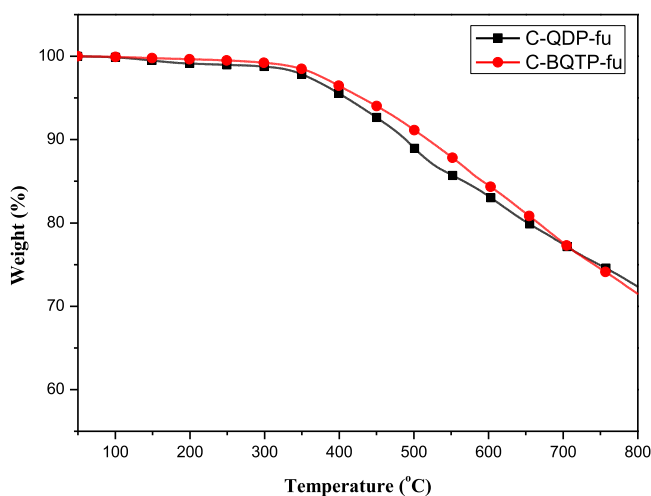
3. CONCLUSIONS

We have successfully prepared a quinoxaline-containing diphenol (QDP) and tetraphenol (BQTP). Based on QDP and BQTP, we have successfully prepared two benzoxazines (QDP-fu and BQTP-fu) from the Mannich condensation of furfurylamine, formaldehyde, with QDP and BQTP, respectively, in a co-solvent of xylene/pentanol (2/1, v/v) at 120 °C. ¹H and ¹³C, ¹H–¹H, and ¹H–¹³C NMR spectra have successfully confirmed their structures. Through IR analysis, we found that the curing reactions include a sequential curing procedure. The ring opening of oxazine and the reaction of furan with zwitterion of oxazine take place at the early stage of curing, and the reaction of free ortho with zwitterion of oxazine take place later. Thermal analysis shows that the thermosets (C-QDP-fu and C-BQTP-fu) exhibit very high thermal properties. Especially, C-BQTP-fu showed impressive thermal properties, with a T_g value of 418 °C, a CTE of 39 ppm/°C, a

Table 2. Thermal Properties of Thermosets of the Benzoxazines

sample code	T_g (°C) ^a (DMA)	T_g (°C) ^b (TMA)	CTE ^c (ppm/°C)	E' ^d (GPa)	T_{ds} ^e (°C)	T_{d10} ^f (°C)	char yield ^g (%)
C-QDP-fu	329	268	58	1.3	410	486	72
C-BQTP-fu	419	295	39	4.0	430	519	72

^aMeasured by DMA at a heating rate of 5 °C/min. ^bMeasured by TMA at a heating rate of 5 °C/min. ^cCTE, recorded from 50 to 150 °C. ^dStorage modulus (E') is recorded at 50 °C. ^eTemperature corresponding to 5% weight loss by thermogravimetry at a heating rate of 20 °C/min. ^fTemperature corresponding to 10% weight loss by thermogravimetry at a heating rate of 20 °C/min. ^gResidual wt % at 800 °C.

**Figure 12.** DMA thermograms of C-QDP-fu and C-BQTP-fu.**Figure 13.** TGA thermogram of C-QDP-fu and C-BQTP-fu.

5% decomposition temperature of 430 °C, and a char yield of 72%. To the best of our knowledge, these properties are competitive to other polybenzoxazines.

4. EXPERIMENTAL SECTION

4.1. Materials. 4,4'-Dimethoxybenzil (from Alfa), pyridine hydrochloride (from Alfa), *o*-phenylenediamine (from Alfa), furfurylamine (from Aldrich), paraformaldehyde (from Acros), and 3,3-diamionbenzidine (from Acros) are used as received. *N*-Methyl pyrrolidone (HPLC grade from Showa) and *N,N*-dimethyl acetamide (DMAc, HPLC grade from Showa) were purified by distillation under reduced pressure over calcium hydride (from Acros), and stored over molecular sieves. The other solvents are (HPLC grade) and used without further purification.

4.2. Characterization. DMA was measured using a PerkinElmer Pyris Diamond DMA with a sample size of 5.0 cm in length, 1.0 cm in width, and around 25 μ m in thickness. The storage modulus E' and $\tan \delta$ were determined as the sample was subjected to the temperature scan mode with a rate of 5 °C/min at a frequency of 1 Hz. The test was performed using a tension mode with an amplitude of 25 μ m. TMA was performed using an SII TMA/SS6100 with a heating rate of 5 °C/min. The sample size is the same as the DMA measurement. The CTE was recorded at the temperature range of 50–150 °C. TGA was performed with a PerkinElmer Pyris1 at a heating rate of 20 °C/min under an atmosphere of nitrogen or air. DSC scans were obtained using a PerkinElmer DSC 8000 in a nitrogen atmosphere with a heating rate of 10 °C/min. NMR measurements (¹H NMR, ¹³C NMR, 2D COSY (¹H–¹H) and 2D HETCOR (¹H–¹³C)) were performed using a Varian Inova 600 NMR in DMSO-*d*₆. IR spectra were obtained from KBr pallet (concentration 1/100 w/w) at least 32 scans in the standard wavenumber range of 667–4000 cm⁻¹ using a PerkinElmer RX1 infrared spectrophotometer.

4.3. Synthesis of 4,4-Dihydroxybenzil. 4,4-Dihydroxybenzil was prepared from demethylation of 4,4'-dimethoxybenzil, according to the literature.⁴⁵ Light yellow powder with 91% yield was obtained. ¹H NMR (ppm, DMSO-*d*₆): δ = 6.90 (4H, H₄), 7.73 (4H, H₃), 10.81 (2H, OH).

4.4. Synthesis of 4,4'-(Quinoxaline-2,3-diyl)diphenol (QDP). QDP was prepared according to the following procedure. *o*-Phenylenediamine 0.67 g (6.2 mmol), 4,4-dihydroxybenzil 1.5 g (6.2 mmol), and toluene/acetic acid (1/2, v/v) 30 mL were introduced into a 100 mL round-bottom glass flask equipped with a condenser and a magnetic stirrer. The solution was stirred at 110 °C for 8 h. The solution was then distilled to remove toluene and poured into water to remove acetic acid. The precipitate was washed by water twice. After drying, yellow powder with a yield of 88% was obtained. ¹H NMR (ppm, DMSO-*d*₆): δ = 6.75 (4H, H₇), 7.33 (4H, H₆), 7.74 (2H, H₂), 8.03 (2H, H₁), 9.77 (2H, OH). ¹³C NMR (ppm, DMSO-*d*₆): δ = 114.9 (C⁷), 128.5 (C¹), 129.6 (C⁴), 129.7 (C²), 131.1 (C⁶), 140.2 (C³), 152.8 (C⁵), 158.1 (C⁸).

4.5. Synthesis of 4,4',4'',4'''-[(6,6'-Biquinoxaline)-2,2',3,3'-tetrayl]tetraphenol. BQTP was prepared according to the following procedure. 3,3-Diamionbenzidine 0.664 g (3.1 mmol), 4,4-dihydroxybenzil 1.5 g (6.2 mmol), and toluene/acetic acid (1/2, v/v) 30 mL were introduced into a 100 mL round-bottom glass flask equipped with a condenser and a magnetic stirrer. The solution was stirred at 110 °C for 8 h. The solution was then distilled to remove toluene and poured into water to remove acetic acid. The precipitate was washed by water twice. After drying, yellow powder with a yield of 88% was obtained. ¹H NMR (ppm, DMSO-*d*₆): δ = 6.75 (8H, H₇), 7.34 (8H, H₆), 8.07 (2H, H₂), 8.22 (2H, H₁), 8.42 (2H, H₁₃), 9.79 (4H, OH). ¹³C NMR (ppm, DMSO-*d*₆): δ = 114.9 (C⁷), 126.2 (C¹³), 128.7 (C¹), 129.1 (C²), 129.6

(C¹⁴), 131.2 (C⁶), 139.6 (C³), 139.9 (C⁴), 140.4 (C¹¹), 152.9 (C⁵), 153.3 (C¹²), and 158.2 (C⁸).

4.6. Synthesis of QDP/Furfurylamine-Based Benzoxazine (QDP-fu). QDP 0.695 g (2.21 mmol), paraformaldehyde 0.266 g (8.84 mmol), furfurylamine 0.429 g (4.42 mmol) and xylene/1-pentanol (2/1) 9 mL were introduced into a 100 mL round-bottom glass flask equipped with a condenser and a magnetic stirrer. The mixture was stirred at 130 °C for 24 h. After that, the solution was poured into hexane to precipitate. The precipitate was dissolved in dichloromethane and extracted with 1.0 N NaOH(aq) twice, and water twice. The organic phase was evaporated to afford light yellow powder with a yield of 81%. ¹H NMR (ppm, DMSO-*d*₆): δ = 3.84 (4H, H13), 3.87 (4H, H11), 4.89 (4H, H12), 6.27 (2H, H17), 6.41 (2H, H16), 6.73 (2H, H7), 7.19 (2H, H6), 7.21 (2H, H10), 7.60 (2H, H15), 7.78 (2H, H2), 8.05 (2H, H1). ¹³C NMR (ppm, DMSO-*d*₆): δ = 47.4 (C¹³), 48.5 (C¹¹), 82.0 (C¹²), 108.7 (C17), 110.4 (C16), 115.5 (C7), 119.4 (C9), 128.5 (C1), 129.2 (C6), 129.3 (C10), 129.8 (C2), 130.9 (C4), 140.2 (C3), 142.7 (C15), 151.5 (C5), 152.4 (C14), and 154.3 (C8). A melting peak at 65 °C, and an exothermic peak at 235 °C with an enthalpy of 309 J/g (359 kJ/mol) were observed in the DSC thermogram.

4.7. Synthesis of BQTP/Furfurylamine-Based Benzoxazine (BQTP-fu). BQTP 0.695 g (2.21 mmol), paraformaldehyde 0.266 g (8.84 mmol), furfurylamine 0.43 g (4.42 mmol), and xylene/1-pentanol (2/1) 9 mL were introduced into a 100 mL round-bottom glass flask equipped with a condenser and a magnetic stirrer. The mixture was stirred at 130 °C for 24 h. After that, the solution was poured into hexane to precipitate. The precipitate was dissolved in dichloromethane and extracted with 1.0 N NaOH(aq) twice, and water twice. The organic phase was evaporated to afford yellow powder with a yield of 76%. ¹H NMR (ppm, DMSO-*d*₆): δ = 3.82 (16H, H17,15), 4.87 (8H, H16), 6.26 (4H, H21), 6.40 (4H, H20), 6.70 (4H, H7), 7.16 (4H, H6,10), 7.60 (4H, H19), 8.06 (2H, H2), 8.20 (2H, H1), 8.40 (2H, H13). ¹³C NMR (ppm, DMSO-*d*₆): δ = 47.4 (C¹⁷), 48.5 (C¹⁵), 82.0 (C¹⁶), 108.7 (C²¹), 110.4 (C²⁰), 115.5 (C⁷), 119.4 (C⁹), 126.3 (C¹³), 128.9 (C^{6,2,1,10}), 130.8 (C¹⁴), 139.9 (C^{4,3,11}), 142.7 (C¹⁹), 151.5 (C⁵), 152.4 (C¹⁸), 152.8 (C¹²), and 154.4 (C⁸). A melting peak at 102 °C, and an exothermic peak at 225 °C with an enthalpy of 223 J/g (172 kJ/mol) were observed in the DSC thermogram.

4.8. Sample Preparation and Curing Procedure. QDP-fu and BQTP-fu were dissolved in DMAc to make a solution with a solid content of 20 wt %. The solution was cast in an aluminum mold, and dried in an oven at 80 °C for 12 h to remove most of the solvent, and then cured at 140, 200, and 240 °C (2 h for each temperature). The thermosetting film is named C-QDP-fu and C-BQTP-fu, in which C represents cured.

AUTHOR INFORMATION

Corresponding Authors

*E-mail: tyjuang@mail.cmu.edu.tw (T.-Y.J.).

*E-mail: lynch@nchu.edu.tw (C.-H.L.).

ORCID

Mahdi M. Abu-Omar: 0000-0002-4412-1985

Ching-Hsuan Lin: 0000-0003-0381-2736

Notes

The authors declare no competing financial interest.

ACKNOWLEDGMENTS

This work was financially supported by the “Advanced Research Center For Green Materials Science and Technology” from The Featured Area Research Center Program within the framework of the Higher Education Sprout Project by the Ministry of Education (107L9006) and the Ministry of Science and Technology in Taiwan (MOST 107-3017-F-002-001 and 107-2221-E-005-026).

REFERENCES

- (1) Mirjalili, B. B. F.; Akbari, A. Nano-TiO₂: an eco-friendly alternative for the synthesis of quinoxalines. *Chin. Chem. Lett.* **2011**, *22*, 753–756.
- (2) Climent, M. J.; Corma, A.; Hernández, J. C.; Hungria, A. B.; Iborra, S.; Martínez-Silvestre, S. Biomass into chemicals: one-pot two- and three-step synthesis of quinoxalines from biomass-derived glycols and 1, 2-dinitrobenzene derivatives using supported gold nanoparticles as catalysts. *J. Catal.* **2012**, *292*, 118–129.
- (3) Venuti, M. C. 2, 3-Dihydroxy-1, 4-dioxane: a stable synthetic equivalent of anhydrous glyoxal. *Synthesis* **1982**, *1982*, 61–63.
- (4) Stille, J. K.; Williamson, J. R. Polyquinoxalines. *J. Polym. Sci., Part A: Gen. Pap.* **1964**, *2*, 3867–3875.
- (5) Hergenrother, P. M.; Levine, H. H. Phenyl-substituted polyquinoxalines. *J. Polym. Sci., Part A-1: Polym. Chem.* **1967**, *5*, 1453–1466.
- (6) Xu, F.; Cheng, G.; Hao, H.; Wang, Y.; Wang, X.; Chen, D.; Peng, D.; Liu, Z.; Yuan, Z.; Dai, M. Mechanisms of Antibacterial Action of Quinoxaline 1, 4-di-N-oxides against *Clostridium perfringens* and *Brachyspira hyodysenteriae*. *Front. Microbiol.* **2016**, *7*, 1948.
- (7) Loughran, H. M.; Han, Z.; Wrobel, J. E.; Decker, S. E.; Ruthel, G.; Freedman, B. D.; Hart, R. N.; Reitz, A. B. Quinoxaline-based inhibitors of Ebola and Marburg VP40 egress. *Bioorg. Med. Chem. Lett.* **2016**, *26*, 3429–3435.
- (8) Guirado, A.; Sánchez, J. I. L.; Ruiz-Alcaraz, A. J.; Bautista, D.; Gálvez, J. Synthesis and biological evaluation of 4-alkoxy-6, 9-dichloro [1, 2, 4] triazolo [4, 3-a] quinoxalines as inhibitors of TNF- α and IL-6. *Eur. J. Med. Chem.* **2012**, *54*, 87–94.
- (9) Zghaib, Z.; Guichou, J.-F.; Vappiani, J.; Bec, N.; Hadj-Kaddour, K.; Vincent, L.-A.; Paniagua-Gayraud, S.; Larroque, C.; Moarbes, G.; Cuq, P.; Kassab, I.; Deleuze-Masquéfa, C.; Diab-Assaf, M.; Bonnet, P.-A. New imidazoquinoxaline derivatives: Synthesis, biological evaluation on melanoma, effect on tubulin polymerization and structure–activity relationships. *Bioorg. Med. Chem.* **2016**, *24*, 2433–2440.
- (10) Ghattass, K.; El-Sitt, S.; Zibara, K.; Rayes, S.; Haddadin, M. J.; El-Sabban, M.; Gali-Muhtasib, H. The quinoxaline di-N-oxide DCQ blocks breast cancer metastasis in vitro and in vivo by targeting the hypoxia inducible factor-1 pathway. *Mol. Cancer* **2014**, *13*, 12.
- (11) Deady, L. W.; Kaye, A. J.; Finlay, G. J.; Baguley, B. C.; Denny, W. A. Synthesis and Antitumor Properties of N-[2-(Dimethylamino)ethyl]carboxamide Derivatives of Fused Tetracyclic Quinolines and Quinoxalines: A New Class of Putative Topoisomerase Inhibitors. *J. Med. Chem.* **1997**, *40*, 2040–2046.
- (12) Noolvi, M. N.; Patel, H. M.; Bhardwaj, V.; Chauhan, A. Synthesis and in vitro antitumor activity of substituted quinazoline and quinoxaline derivatives: search for anticancer agent. *Eur. J. Med. Chem.* **2011**, *46*, 2327–2346.
- (13) Corona, P.; Carta, A.; Loriga, M.; Vitale, G.; Paglietti, G. Synthesis and in vitro antitumor activity of new quinoxaline derivatives. *Eur. J. Med. Chem.* **2009**, *44*, 1579–1591.
- (14) Ning, X.; Ishida, H. Phenolic materials via ring-opening polymerization: Synthesis and characterization of bisphenol-A based benzoxazines and their polymers. *J. Polym. Sci., Part A: Polym. Chem.* **1994**, *32*, 1121–1129.
- (15) Ishida, H.; Low, H. Y. A Study on the Volumetric Expansion of Benzoxazine-Based Phenolic Resin. *Macromolecules* **1997**, *30*, 1099–1106.
- (16) Puchot, L.; Verge, P.; Peralta, S.; Habibi, Y.; Vancaeyzeele, C.; Vidal, F. Elaboration of bio-epoxy/benzoxazine interpenetrating

- polymer networks: a composition-to-morphology mapping. *Polym. Chem.* **2018**, *9*, 472–481.
- (17) Zhang, S.; Ran, Q.; Fu, Q.; Gu, Y. Preparation of Transparent and Flexible Shape Memory Polybenzoxazine Film through Chemical Structure Manipulation and Hydrogen Bonding Control. *Macromolecules* **2018**, *51*, 6561–6570.
- (18) Kaya, G.; Kiskan, B.; Yagci, Y. Phenolic Naphthoxazines as Curing Promoters for Benzoxazines. *Macromolecules* **2018**, *51*, 1688–1695.
- (19) Salum, M. L.; Iguchi, D.; Arza, C. R.; Han, L.; Ishida, H.; Froimowicz, P. Making Benzoxazines Greener: Design, Synthesis, and Polymerization of a Biobased Benzoxazine Fulfilling Two Principles of Green Chemistry. *ACS Sustainable Chem. Eng.* **2018**, *6*, 13096–13106.
- (20) Iguchi, D.; Ohashi, S.; Abarro, G. J. E.; Yin, X.; Winroth, S.; Scott, C.; Gleydura, M.; Jin, L.; Kanagasegar, N.; Lo, C.; Arza, C. R.; Froimowicz, P.; Ishida, H. Development of Hydrogen-Rich Benzoxazine Resins with Low Polymerization Temperature for Space Radiation Shielding. *ACS Omega* **2018**, *3*, 11569–11581.
- (21) Ishida, H.; Agag, T. *Handbook of Benzoxazine Resins*; Elsevier, 2011.
- (22) Ishida, H.; Froimowicz, P. *Advanced and Emerging Polybenzoxazine Science and Technology*; Elsevier, 2017.
- (23) Wang, J. Monoamine - monophenol type quinoxaline phenyl oxazine and its preparation method. China patent no. CN105153194B, 2015.
- (24) Wang, J. Monophenols - monoamines type quinoxaline phenyl benzoxazine and preparation method. China patent no. CN105111199B, 2015.
- (25) Wang, J. Quinoxaline type triamine benzene and oxazine and its preparation method. China patent no. CN105130975B 2015.
- (26) Agag, T.; Takeichi, T. High-molecular-weight AB-type benzoxazines as new precursors for high-performance thermosets. *J. Polym. Sci., Part A: Polym. Chem.* **2007**, *45*, 1878–1888.
- (27) Chang, C. W.; Lin, C. H.; Lin, H. T.; Huang, H. J.; Hwang, K. Y.; Tu, A. P. Development of an aromatic triamine-based flame-retardant benzoxazine and its high-performance copolybenzoxazines. *Eur. Polym. J.* **2009**, *45*, 680–689.
- (28) Lin, C. H.; Chang, S. L.; Hsieh, C. W.; Lee, H. H. Aromatic diamine-based benzoxazines and their high performance thermosets. *Polymer* **2008**, *49*, 1220–1229.
- (29) Adams, R.; Voorhees, V. Furfural. *Org. Synth.* **1921**, *1*, 49.
- (30) Peters, F. N., Jr The Furans: Fifteen Years of Progress. *Ind. Eng. Chem.* **1936**, *28*, 755–759.
- (31) Liu, Y.-L.; Chou, C.-I. High performance benzoxazine monomers and polymers containing furan groups. *J. Polym. Sci., Part A: Polym. Chem.* **2005**, *43*, 5267–5282.
- (32) Trejo-Machin, A.; Verge, P.; Puchot, L.; Quintana, R. Phloretic acid as an alternative to the phenolation of aliphatic hydroxyls for the elaboration of polybenzoxazine. *Green Chem.* **2017**, *19*, 5065–5073.
- (33) Wang, C.; Sun, J.; Liu, X.; Sudo, A.; Endo, T. Synthesis and copolymerization of fully bio-based benzoxazines from guaiacol, furfurylamine and stearylamine. *Green Chem.* **2012**, *14*, 2799–2806.
- (34) Sini, N. K.; Bijwe, J.; Varma, I. K. Renewable benzoxazine monomer from Vanillin: Synthesis, characterization, and studies on curing behavior. *J. Polym. Sci., Part A: Polym. Chem.* **2014**, *52*, 7–11.
- (35) Dumas, L.; Bonnaud, L.; Olivier, M.; Poorteman, M.; Dubois, P. High performance bio-based benzoxazine networks from resorcinol and hydroquinone. *Eur. Polym. J.* **2016**, *75*, 486–494.
- (36) Dumas, L.; Bonnaud, L.; Olivier, M.; Poorteman, M.; Dubois, P. Arbutin-based benzoxazine: en route to an intrinsic water soluble biobased resin. *Green Chem.* **2016**, *18*, 4954–4960.
- (37) Dai, J.; Teng, N.; Peng, Y.; Liu, Y.; Cao, L.; Zhu, J.; Liu, X. Biobased Benzoxazine Derived from Daidzein and Furfurylamine: Microwave-Assisted Synthesis and Thermal Properties Investigation. *ChemSusChem* **2018**, *11*, 3175–3183.
- (38) Brunovska, Z.; Liu, J. P.; Ishida, H. 1,3,5-Triphenylhexahydro-1,3,5-triazine—active intermediate and precursor in the novel synthesis of benzoxazine monomers and oligomers. *Macromol. Chem. Phys.* **1999**, *200*, 1745–1752.
- (39) Lin, C. H.; Chang, S. L.; Shen, T. Y.; Shih, Y. S.; Lin, H. T.; Wang, C. F. Flexible polybenzoxazine thermosets with high glass transition temperatures and low surface free energies. *Polym. Chem.* **2012**, *3*, 935–945.
- (40) Wang, C.; Zhao, C.; Sun, J.; Huang, S.; Liu, X.; Endo, T. Synthesis and thermal properties of a bio-based polybenzoxazine with curing promoter. *J. Polym. Sci., Part A: Polym. Chem.* **2013**, *51*, 2016–2023.
- (41) Li, S.; Yan, S. Synthesis and characterization of novel biobased benzoxazines from cardbisphenol and the properties of their polymers. *RSC Adv.* **2015**, *5*, 61808–61814.
- (42) Agag, T.; Takeichi, T. Synthesis and Characterization of Novel Benzoxazine Monomers Containing Allyl Groups and Their High Performance Thermosets. *Macromolecules* **2003**, *36*, 6010–6017.
- (43) Ning, X.; Ishida, H. Phenolic materials via ring-opening polymerization: Synthesis and characterization of bisphenol-A based benzoxazines and their polymers. *J. Polym. Sci., Part A: Polym. Chem.* **1994**, *32*, 1121–1129.
- (44) Liu, J.; Ishida, H. Anomalous Isomeric Effect on the Properties of Bisphenol F-based Benzoxazines: Toward the Molecular Design for Higher Performance. *Macromolecules* **2014**, *47*, 5682–5690.
- (45) Jarvid, M.; Johansson, A.; Bjuggren, J. M.; Wutzel, H.; Englund, V.; Gubanski, S.; Müller, C.; Andersson, M. R. Tailored side-chain architecture of benzil voltage stabilizers for enhanced dielectric strength of cross-linked polyethylene. *Journal of Polymer Science Part B: Polymer Physics* **2014**, *52*, 1047–1054.